The Tony Davies High Voltage Laboratory

UNIVERSITY OF Southampton

Deliverable Report

Report issued to:
ORE Catapult

Offshore House, Albert Street, Blyth,
Northumberland, NE24 1LZ

Project: Offshore Wind Cable Catalogue

Contact: Hytham Emam
Email: hytham.emam@ore.catapult.org.uk
Phone: +44 01670 357625

Deliverable Number: 2.0
Ref: ORE/15/57
TDHVL Ref: 15242-RE2-v7

The continuous thermal rating for a range of typical 132kV 3 phase SL type cables have been investigated for a series of installation environments, including:

- Burial in sea bed at depths of 1m and 3m
- Burial in ducted HDD at landfall
- J Tube between off shore platform and sea bed

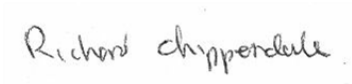
The continuous ratings have been calculated with both standard analytical approaches and bespoke finite element analysis models which are better able to represent complex thermal environments. Included within the FEA approach are an updated set of induced losses which are believed to more accurately account for the thermal losses within this type of cable.

Document Originator:
The Tony Davies High Voltage Laboratory
Building 20, University Crescent
Electronics and Electrical Engineering
Faculty of Physical Science & Engineering
University of Southampton
Southampton, SO17 1BJ
UK

Tel: 023 8059 4450
Fax: 023 8059 3709

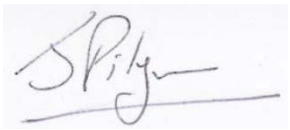
Email: pll@ecs.soton.ac.uk
Contact: Prof Paul Lewin

Report prepared by:



Dr Richard Chippendale

Reviewed by:



Dr James Pilgrim MIEEE

Date: 14/10/2016

Executive Summary

The continuous thermal rating for the following selection of 3 phase SL type wind farm export cable have been investigated:

- 800 mm^2 Copper conductor at 132 kV
- 1600 mm^2 Aluminium conductor at 220 kV
- 2000 mm^2 Aluminium conductor at 220 kV
- 2000 mm^2 Copper conductor at 220 kV
- 2000 mm^2 Aluminium conductor at 275 kV
- 2000 mm^2 Copper conductor at 275 kV

Using these cable designs the continuous thermal ratings have been calculated in the following installation environments:

- Burial in sea bed at depths of 1m and 3m
- Burial in ducted HDD at landfall
- J Tube between off shore platform and sea bed

The continuous ratings for these environments have been calculated with both the internationally standard analytical approaches of IEC 60287 and a bespoke finite element analysis (FEA) approach which allows for an improved representation of the cable thermal design and the installation environment. Included within the FEA approach are an updated set of induced losses (in the sheaths and armour) which are believed to more accurately account for the thermal losses within this type of cable than the equations given in IEC 60287.

The predicted continuous ratings for the 800 mm^2 cable has initially been considered in detail for each considered method and installation environment as is presented in Table 1.

Table 1 – Comparison of continuous rating methods

Installation environment	Continuous Ratings [A]			% gain between standard method and FEA with advanced losses
	Standard methods	FEA with IEC losses	FEA with advanced losses	
Typical seabed burial	896	893	925	3.2
Deep seabed burial	811	811	847	4.4
HDD Landfall	598	605	644	7.7
J tube	835	893	928	11

The above table shows that the HDD landfall always has the lowest continuous rating regardless of method given the large depth of burial. The least thermally limiting sections in this case study are those where the cable is buried in the sea bed.

By developing a bespoke FEA model and considering the induced losses according to the approach published in [1], rating increases of up to 7.7% are obtained in comparison to the standard IEC methods. The improvement in rating decreases as the burial depth of the cable decreases owing to the rating being dominated by the close proximity of the sea bed boundary. Such a large increase in rating is apparent due to the considerable reduction in armour loss within the method by [1]. *Since the permeability of steel is dependent on the composition and manufacturing processes, it is suggested that the permeability is verified, as the armour loss factor will impact the continuous thermal rating. This represents a key*

uncertainty when comparing different cable types.

There is a more significant increase in rating between the classical method and the bespoke FEA method for the J tube. This is caused by both the improved loss prediction and also the improved modelling of the heat transfer within a J tube, which the FEA model allows.

Having considered the continuous ratings for the 800 mm^2 in detail, the study has then been repeated for each of the remaining cable designs. By comparing the rating for the larger conductor sizes, it was found that the aluminium conductors have approximately a 7% decrease in rating with IEC losses and a 9% lower rating with advanced losses, as compared with the rating from a copper conductor of the same size.

Furthermore it has been shown that when considering the IEC thermal losses, there is a decrease in rating by replacing half of the steel armour wires with polymer. This is believed not to be physical and is a limitation of the assumptions made within the IEC approach. This issue is not present with the advanced losses as a rating increase has been observed. This further illustrates the importance of using the advanced thermal losses for a SL type cable over the standard IEC approach.

The study has shown that the percentage rating increase for a Milliken conductor is slightly greater when using the advanced losses (maximum of approx. 10% at typical burial depth) than for the IEC losses (maximum of approx. 8% at typical burial depth). Furthermore it is evident that as the burial depth of the cable increases the percentage increase in rating, decreases. This is expected due to the increased dominance of the external soil on the rating as the depth increases.

By comparing the ratings for the various proposed conductor sizes, the report has demonstrated that at a fixed operating voltage, the continuous rating increases with increasing conductor size, as expected. Further, when considering the same conductor size, there is a decrease in continuous rating with increased operating voltage. This is due to the increased insulation thickness required for higher voltages, and an increased dielectric thermal loss. Finally, the results have also shown that when comparing an aluminum or a copper conductor, if the cables are operating at the same voltage and have the same cross sectional area, the copper conductor will have a higher rating than the aluminum conductor. This rating difference is due to the lower electrical resistance of the copper.

Contents

Executive Summary **2**

1.0 Introduction **6**

1.1 Cable design *6*

1.1.1 Cable design assumptions 9

1.2 Circuit installation environments *9*

1.2.1 Typical Seabed Burial 9
1.2.2 Deep Seabed Burial 10
1.2.3 Typical Landfall 10
1.2.4 J Tube 11

2.0 Continuous Ratings Using Standard Approaches **13**

2.1 IEC thermal network *13*

2.2 ERA J tube Method *13*

2.3 Discussion *14*

3.0 Continuous Ratings from Advanced Methods **15**

3.1 Finite Element Analysis *15*

3.1.1 Buried cables 15
3.1.2 J tube models 16

3.2 Improved Models of Induced Losses *17*

3.3 Discussion *19*

4.0 Continuous Ratings for Remaining Cables **22**

4.1 Thermal Rating for remaining cables *22*

4.2 Effect of Milliken Conductor Design *24*

5.0 Conclusions **25**

6.0 References **28**

7.0 Appendix **29**

7.1 132kV 800 mm^2 copper conductor *29*

7.2 220kV 1600 mm^2 Aluminium conductor *30*

7.3 220kV 2000 mm^2 Aluminium conductor *31*

7.4 220kV 2000mm^2 copper conductor *32*

7.5 275kV 2000 mm^2 Aluminium conductor *33*

7.6 275kV 2000 mm^2 copper conductor *34*

Appendix B: 35

1.0 Introduction

The aim of this project is to investigate the specification of large cables that have the potential to be used within larger scale Offshore Wind Installations. The first phase of this project is to define a range of appropriate cable dimensions, based upon a collection of reference designs and then predict the continuous thermal rating using the base case cable design (132 kV with 800 mm^2 copper conductor) for a series of installation environments. The generic form of the reference cable is:

- 132 kV 3 phase SL type
- Conductor: 800 mm^2 copper, plain stranded wires
- Insulation: cross-linked polyethylene (XLPE)
- Sheath: Lead
- Armour: single layer of (standard galvanized) steel wires
- Interstices: mixture of polypropylene yarn and air

Using the 800 mm^2 as the base case the second phase of this project considers the potential increase in rating of using the following larger cables:

- 1600 mm^2 Aluminium conductor at 220 kV
- 2000 mm^2 Aluminium conductor at 220 kV
- 2000 mm^2 Copper conductor at 220 kV
- 2000 mm^2 Aluminium conductor at 275 kV
- 2000 mm^2 Copper conductor at 275 kV

The dimensions of the larger cable sizes are based on the same layer thicknesses as that from the 800 mm^2 cable. The only exception to this is that the insulation around each core should be defined with reference to the electric field strength. If the electric field strength of the 800 mm^2 cable was used with the larger conductors' sizes, the cable would have an excessively thick insulation layer (significantly reducing minimum bend radius). Therefore for conductor sizes greater than 800 mm^2 a target stress of 8.5 $kVmm^{-1}$ has been defined. This represents a reasonable stress level for existing designs [2], although it may be slightly conservative for the 275 kV options. The incurred conservatism in the rating will not be significant, due to an extra millimetre of insulation thickness. Using the target stress level the insulation thickness of each cable design has been varied to the nearest half millimetre to achieve the best agreement with the target stress. Hence, the quoted stress in Appendix A for each cable design might be slightly above or below the target stress, due to the rounding of the insulation thickness.

For conductor sizes greater than 800 mm^2, the armour is comprised of 50% steel and 50% polymeric wires. To increase the continuous ratings, those conductors which have a cross sectional area of 2000 mm^2 are considered to have an insulated Milliken design, as compared to the smaller cables which have a plain stranded design. A summary of all reference cable designs to be studied throughout this work is included in Appendix A.

The initial section of this report considers the continuous rating of the 132 kV cable with 800 mm^2 copper conductor within the stated installation environments. Once these ratings have been considered in detail, the study is repeated to consider the remaining larger conductor sizes.

The remainder of this section present the 800 mm^2 cable design in more detail (Section 1.1), followed by the layout of the installation environments (Section 1.2).

1.1 Cable design

An illustration of the typical cable geometry is presented in Figure 1.

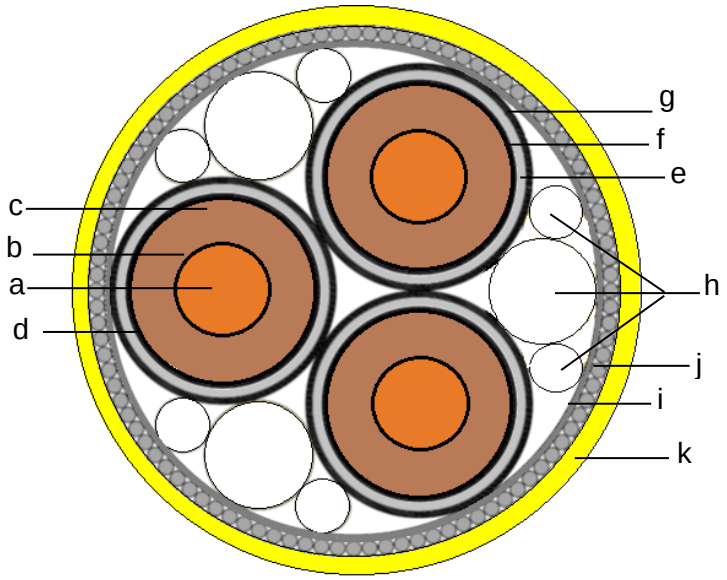


Figure 1- Illustration of typical 3 core SL type cable

The regions defined in Figure 1 are explained along with their construction material and dimensions in Table 2.

Table 2 - Cable components and dimensions for 132kV 800 mm^2 copper cable

Label	Component Name	Material	Outer Diameter [mm]	Thickness [mm]
a	Conductor	Copper	34.5	
b	Conductor screen	Semiconducting polymer	37.5	1.5
c	Insulation	XLPE	71.5	17
d	Insulation screen	Semiconducting polymer	74.5	1.5
e	Swelling Tape	Semiconducting water blocking tape	77.5	1.5
f	Sheath	Lead alloy	82.5	2.5
g	Power core oversheath	Polyethylene	87.0	2.2
h	Fillers	Polypropylene yarn		various
i	Binder tape	Polymeric tape	191.0	2
j	Armour wires	Steel wires with Bitumen	203.0	5.6
k	Outer Serving	Polypropylene yarn with bitumen	212.0	4.5

The thermal conductivity for each material used in the above cable designs are presented in Table 3. These material properties are typical book values from IEC 60287-2 [3]. The additional materials for air and water are not included within [3] and are hence typical book values [4]. The thermal conductivity of the semiconducting polymers used in the conductor and insulation screen is assumed to be the same as the XLPE, as there are no agreed book values. This is slightly conservative as the addition of the electrically conductive filler is likely to increase the bulk thermal conductivity, however the effect on the overall ratings is small. This approach aligns with standard practice for the use of IEC 60287, as the conductor and

insulation screens are considered to be thermally identical to the main insulation wall.

Table 3 - Thermal material properties

Material	Thermal Conductivity ($Wm^{-1}K^{-1}$)
Copper	400
Aluminium	236
XLPE	0.286
Semiconducting Polymer	0.286
Water swellable tape (assumed XLPE)	0.286
Lead	35.3
Polypropylene yarn	0.2
Steel	18
Air	0.0242
Water	0.58

The material properties of the water swellable tape are difficult to characterise. However because it is relatively thin, this layer will not have a significant impact on the thermal profile within the cable, therefore it will be assumed to have the same thermal properties as XLPE.

The electrical material properties for the considered cable designs are presented in Table 4. These values are typical book values taken from [5].

Table 4 - Electrical properties of the cables

Parameter	Value
Electrical resistivity of copper	1.72×10^{-8} Ωm
Copper temperature coef. of resistance	3.93×10^{-3} K^{-1}
Copper conductor kp (plain stranded)	0.8
Copper conductor ks (plain stranded)	1
Copper conductor kp (Insulated Milliken)	0.2
Copper conductor ks (Insulated Milliken)	0.35
Electrical resistivity of Aluminium	2.8×10^{-8} Ωm
Aluminium temperature coef. of resistance	4.03×10^{-3} K^{-1}
Aluminium conductor kp (plain stranded)	1
Aluminium conductor ks (plain stranded)	1
Aluminium conductor kp (Insulated Milliken)	0.15
Aluminium conductor ks (Insulated Milliken)	0.25
Lead sheath Resistivity	2.14×10^{-7} Ωm
Lead sheath temp coef. of resistance	0.004 K^{-1}
Galvanized steel Armour Resistivity	1.38×10^{-7} Ωm
Galvanized steel Armour temp coef. of resistance	$4.50 \times 10^{-3} K^{-1}$
Armour kp	1
Armour ks	1
Relative permittivity of Insulation (XLPE)	2.5
Insulation Tan Delta	0.001
Frequency	50 Hz

The electrical resistance of all metallic components (conductor, sheath and armour) is thermally dependent. To account for this thermal variation the temperature coefficient of resistance of each component is specified in Table 4. Using these terms the predicted rating from each method is calculated with the thermally dependent resistance based on the corresponding calculated temperature.

1.1.1 Cable design assumptions

Before developing the numerical models for the different installation environments, this study first considers if there are any simplifying assumptions which can be made to the cable design. These simplifying assumptions are especially important for 3D finite element models, as poorly designed 3D models can be very computationally demanding and hence slow to solve.

Interstices

The interstices of the cable i.e. the area between the power cores and the armour bedding, are assumed to contain a mixture of polypropylene yarn and air. From experience this yarn is fairly uniformly distributed throughout this region with small air gaps between the individual yarn strands. The empty space between the yarn is assumed to be air rather than water despite considering a subsea cable, because the thermally limiting section is likely to be within the HDD, where the presence of water in the interstices is less likely. In the remaining installation sections the dry filler assumption is carried over, and so will add a degree of conservatism to these ratings. However the rating reduction is not believed to be significant because the majority of the permissible heat flux will be passed through the region where the sheath and armour are closest and hence where there is a minimal amount of filler present.

It is computationally very expensive to directly model each small yarn bundle. However our experience has shown that the most realistic approach to represent this region is to consider it as a single phase solid whose thermal conductivity is estimated through the mixture rule according to the volumetric proportion of air and yarn. This method assumes that there is no thermal convection or radiation between the power cores and the armour bedding. This assumption is sensible for the following reasons:

- The thermal convection within the interstices will be negligible due to the small air gaps between the individual polymer yarns.
- Due to the uniform yarn distributions the radiation heat flux is greatly reduced, and assumed to be minimal.

An exact value for the area of yarns to air within the interstices is not present on the cable datasheet (Appendix A) and so instead it is assumed the interstices is approximately two parts polypropylene to one part air. With this volume fraction and the material thermal conductivities stated in Table 3, the effective thermal conductivity of the interstices are assumed to be 0.123 $Wm^{-1}K^{-1}$. This value will be used for all the other cable designs to be assessed in Phase 2.

1.2 Circuit installation environments

The Scope of Work (SoW) has identified a series of cable installation environments, which are presented in detail within the following section. These installation environments represent the likely thermal conditions that the cable will experience as it passes from an offshore platform to the landfall.

1.2.1 Typical Seabed Burial

The cable environment for a typical sea bed burial is illustrated in Figure 2. This cross

section shows the three phase SL type cable buried at a depth (L_D) of 1 m (to the cable centre) below the sea bed surface.

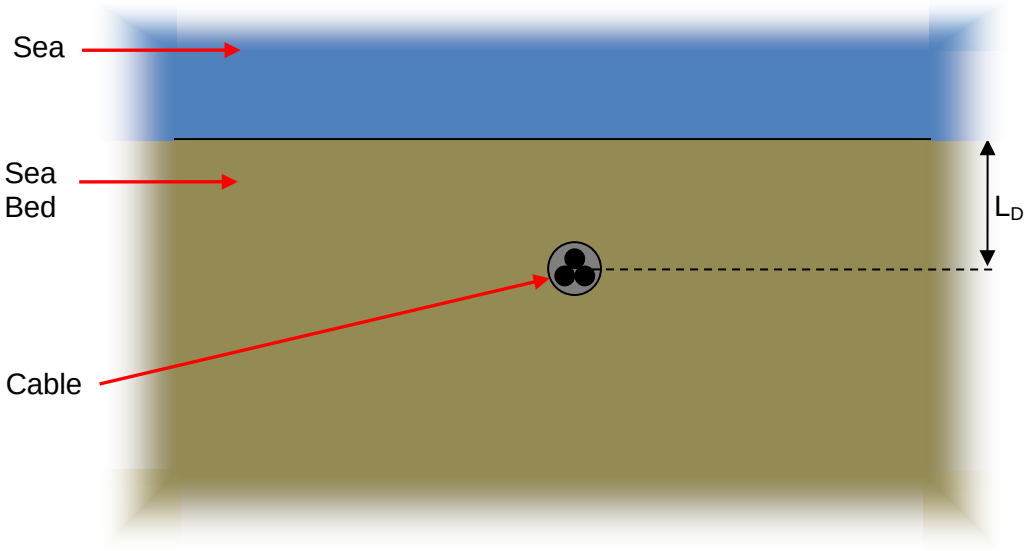


Figure 2 - Illustration of cable buried in sea bed (not to scale)

For this installation environment the thermal resistivity of the sea bed is stated in the SoW to be 0.7 Km/W. The ambient temperature of the sea water is assumed to be 15 °C. Given the high heat transfer coefficient which would be present between the water and the surface of the sea bed, the sea bed surface shall be treated as an isotherm.

1.2.2 Deep Seabed Burial

In some lengths of the sub-sea cable route, it could be necessary to install the cable at greater depths. In addition, some areas of the sea bed are known to contain mobile sediments, with phenomena such as sand waves causing an increase in effective burial depth. As an increase in burial depth will increase the thermal resistance between the cable and the sea water, it will decrease the permissible thermal losses and hence cause a rating decrease. It is therefore important to determine the continuous thermal rating under these installation conditions. The SoW requests that the depth of burial under such conditions be considered to be 3 m.

1.2.3 Typical Landfall

Horizontal directional drilling (HDD) is frequently used to bring the cable in beneath obstacles at the shore line. The depth of burial is often significantly greater than in the sea bed, meaning that the landfall is frequently a thermal pinch point. According to the SoW, the HDD consists of a duct which has an internal diameter of 2.5 times the external diameter of the cable and is backfilled with bentonite to improve the heat transfer. The duct is made from 90 mm thick polyethylene tube. A generic illustration of the HDD is presented in Figure 3.

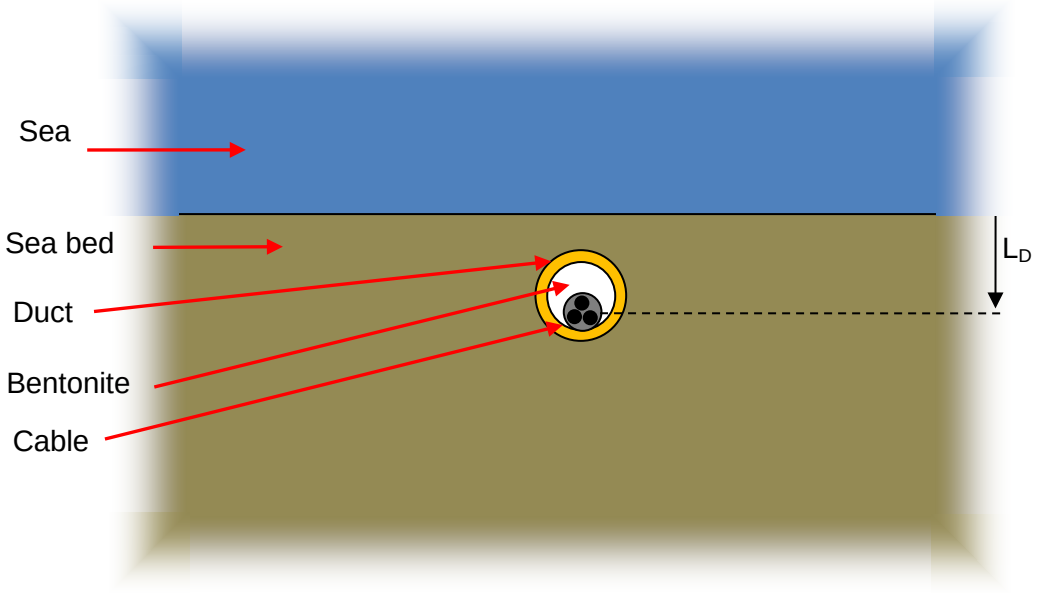


Figure 3 – Cross section perpendicular to cable length of cable within HDD, on the sea side of the landfall

The burial depth of the cable duct varies within this section of the circuit. Starting at the offshore end of the cable length, the initial cable burial depth is 1 m (i.e. typical burial depth). The depth of the cable then linearly increases down to 10.0 m, over a section 66 m long. The cable remains at this maximum burial depth for 200 m. At which point the burial depth decrease linearly back to 1 m over a length of 44 m.

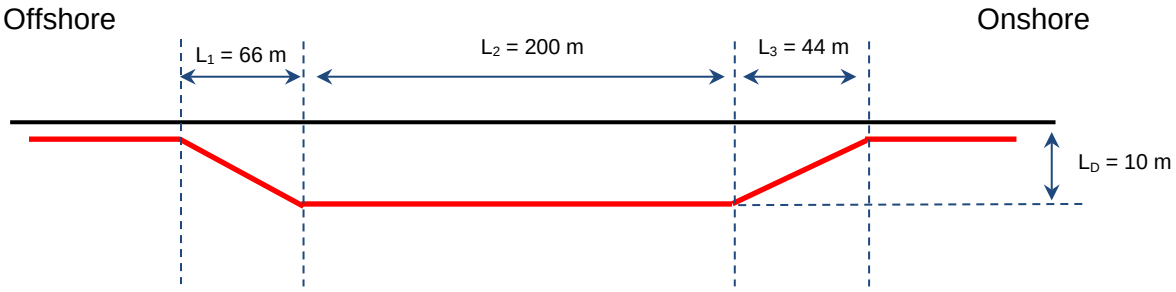


Figure 4 – Illustration of HDD cable depth profile in the landfall section

The thermal resistivity of the soil (on shore) is 1.1 KmW^{-1}, whilst the sea bed thermal resistivity remains at 0.7 KmW^{-1}. The transition in thermal resistivity is assumed to occur in the centre of the deeply buried landfall region. The thermal resistivity of the duct backfill (bentonite) is 1.0 KmW^{-1} and the ambient soil temperature is 15 °C.

In reality the transition in cable profile is limited by a minimum cable bend radius. However given the length of cable considered here, the addition of a smooth bend radius will have minimal impact on the conductor thermal profile and hence a sharp angled transition will be used in the finite element model.

1.2.4 J Tube

The final installation environment which is considered is that of a J tube. A J tube is frequently used as a means for cable protection between an offshore platform and the sea bed. A typical cross section of a J tube is presented in Figure 5, with the key sections being:

- Below sea level, where the gap between the J tube and cable is filled with sea water. This section is referred to as “Tube water section”
- Above sea level but below the offshore platform hang off, where the gap between the J tube and cable is filled with air. This section is referred to as “Tube air section”
- Above the armour hang off, where the individual phases from the export cable are separated and installed in air. This section is referred to by “exposed phases”

The platform hang off is not shown in in Figure 5 because it has not been considered further due its very short length, which means it does not significantly impact the overall temperature profile. This region is likely to be less thermally onerous, due to the large surface area of the hang off, from which heat transferred from the armour wires may be dissipated.

According to the SoW, this study considers a J tube air section length of 15 m high (sea level to deck), which is sealed (i.e. closed) at bottom and top. The steel J tube has a wall thickness of 30 mm and the inner diameter is to be 2.5 times that of the external cable diameter. The tube is not considered to be shielded from the sun by the overhead offshore platform and hence the typical IEC value for solar radiation of 1000 Wm^{-2} will be considered. The solar absorptivity of the external tube surface is assumed to be 0.4. The ambient air temperature is 20 °C and the ambient water temperature is 15 °C.

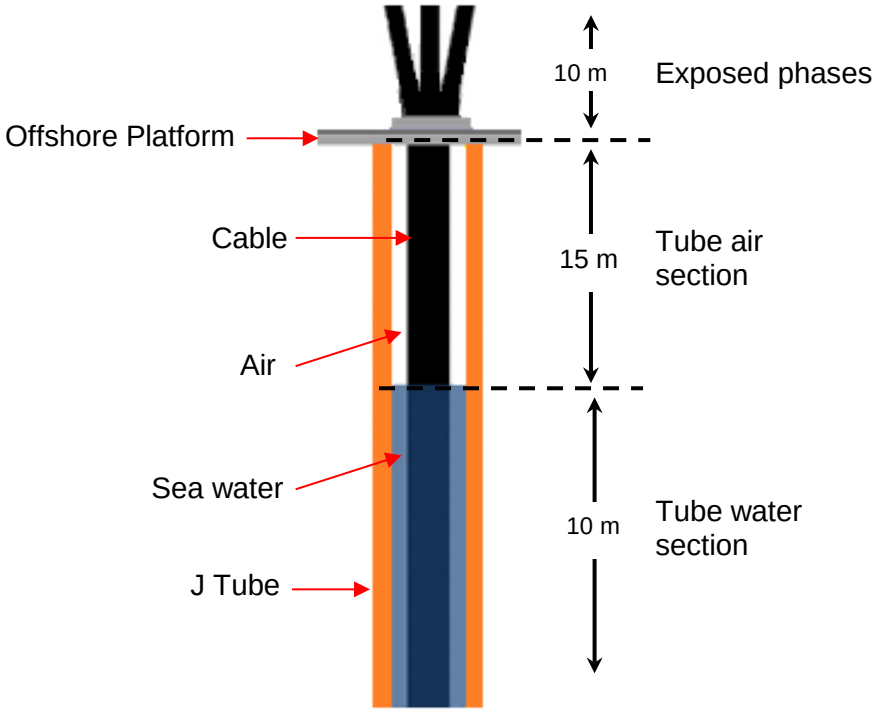


Figure 5 - J tube 3D model

2.0 Continuous Ratings Using Standard Approaches

Before considering any advanced methods to predict the continuous rating for considered installation environment, the ratings have been calculated through standard rating techniques. For the buried cable installations, the IEC 60287 compliant current ratings are given [3] [5]. There is however no internationally standard approach for calculating the continuous thermal rating for a J tube. However there is a simple empirical method proposed by ERA [6], which can be used for J tube ratings. All the thermal ratings will assume a maximum conductor temperature of 90 °C.

2.1 IEC thermal network

For the typically buried (1m depth) and the deeply buried (3m depth) cable, the continuous thermal ratings for buried cables can be calculated from the standard thermal network approach presented in IEC 60287-2 [3], with the cable dimensions and material properties included within Table 2 and Table 3. The thermal losses for the defined thermal network are given by IEC 60287-1 [5], with the electrical parameters presented in Table 4.

However the HDD landfall model is a little more complicated and cannot be directly considered by the standard IEC approach. This is because within the landfall region there is a considerable variation in burial depth, which could result in longitudinal heat transfer and hence a greater rating. To fully account for longitudinal heat transfer a 3D model is required, however the IEC method only considers 2D. To use the IEC approach, it is suggested to take a 2D slice at the centre of the deeply buried section (10m depth). However inherent within this statement is the assumption that there is no longitudinal heat transfer, and so the method may predict a conservative rating if the deep section is suitably short. In addition to the variation in burial depth, the pure IEC 60287 method does not take into account the thermal properties of the duct and its backfill when calculating the continuous rating. To account for these domains two additional thermal resistance terms are required, between the thermal resistance of the armour and soil (T3) and the thermal resistivity of the soil (T4). Using the approach presented in IEC, the thermal resistance for these two regions can be calculated by

$$T = \frac{\rho_k}{2\pi} \ln\left[\frac{r_o}{r_i}\right] \qquad [1]$$

Where ρ_k is the thermal resistivity of material '*k*' and r_i and r_o are the inner and outer radius of the annulus region. This forces the assumption that the cable is centred within the duct, when in reality it is likely to be sitting on the base of the duct, however this is not considered to be a significant source of error.

2.2 ERA J tube Method

Continuous thermal ratings of cables in a J tube are often calculated using an empirically derived method published by ERA in 1988 [6]. When this method was developed, the testing included cable outer diameters between 75 mm and 130 mm and J tubes diameters between 0.16 m and 0.4 m. The cable and J tube diameters considered here are 211 mm and 0.53 m, respectively. These values are greater than the range of the original experimental data, so the results must be used with caution. A review of the method as presented in [6] is given below. *It should be highlighted that modifications to this method are possible (although not presented here) to better align it to the cable model used by the standard IEC 60287 approach. This involves replacing equation 3 in the ERA model with a rearranged version of that for Δθ given in 1.4.1 of IEC 60287-1-1.*

This method predicts the continuous rating by recognizing that under steady state conditions, the permissible heat flux across each radial component must be the same. The

total permissible heat flux through each region, is related to the temperature drop within each region, with the conductor region presented in equation [2], the insulation in equation [3] and the J tube air section by equation [4]

$$W_c = \frac{\Delta\theta_c}{T_T} \quad [2]$$

$$W_i = 20.3\, D_i^{0.315} D_e^{0.73} \Delta\theta_p^{1.05} \quad [3]$$

$$W_e = \pi D_o h_{era} \Delta\theta_s^{1.09} - q_{solar} D_o \alpha \quad [4]$$

Where D_e, D_i and Do are the diameter of cable surface [m], inside J tube surface [m] and outside J tube surface [m]. The temperature difference between the conductor and cable surface is $\Delta\theta_c$ [K], between the cable surface and the tube is $\Delta\theta_p$ [K] and between the tube and the ambient $\Delta\theta_s$ [K]. The total thermal resistivity of the cable is given by T_T [KmW^{-1}] and is calculated by IEC 60287-2 (Note, when summing the total thermal resistance, the thermal resistance T1 should be divide by three if considering a three core cable). The heat transfer coefficient from cable surface is h_{era} [Wm^{-2}K^{-1}], the solar heat flux q_{solar} [Wm^{-2}] and α is the absorptivity.

To complete the above set of equations, the sum of the temperature decrease in each section is defined with respect to the maximum allowed conductor temperature (θ_{max}) minus the ambient temperature ($\Delta\theta_{amb}$), which is expressed as

$$(\theta_{max} - \theta_{amb}) = \Delta\theta_c + \Delta\theta_p + \Delta\theta_s \quad (5)$$

By varying the temperature difference within each region it is possible to obtain the same permissible heat flux through each region. The balanced permissible heat flux solution is then used in conjunction with the thermal losses presented in IEC 60287-1 to calculate the continuous rating required to achieve this permissible heat flux.

2.3 Discussion

Using the above methods the continuous thermal ratings for an 800mm^2 132kV, plain stranded copper conductor in the 4 different installation environments are presented in Table 5.

Table 5 – Continuous thermal rating from standard methods

Environment	Rating [A]
Typical seabed burial	896
Deep seabed burial	811
HDD landfall	598
J tube	835

The ratings presented in Table 5 show that HDD landfall has the lowest continuous rating. Furthermore it is apparent that as the burial depth increases (typical seabed to HDD landfall) the continuous rating decreases. This is expected because an increased burial depth increases the thermal resistance between the cable and the ambient heat sink.

Results for the larger cable sizes are presented in Section 4.

3.0 Continuous Ratings from Advanced Methods

The above section has presented the continuous thermal rating for the considered installation environments using simple analytical and empirical techniques. Whilst these methods are very useful, due to their simple and/or empirical nature, they do not fully consider all the physical processes for more complicated thermal environments or geometry. In order to improve the accuracy of the predicted ratings, a series of 2D and 3D steady state finite element analysis (FEA) models have been developed. The main benefits of using these numerical models are:

- More detailed representation of the cable geometry
- Ability to model the thermal environment of the installation in more detail
- Improved modelling of armour related losses

3.1 Finite Element Analysis

Due to the similarity between several of the installation environments two main categories of numerical models have been developed; buried cables and J tube. Each of these numerical models is described in the following sections.

3.1.1 Buried cables

Using the installation geometries for the typical and deeply buried cable, (Figure 2) a two dimensional cross section model has been implemented within an FEA package. To replicate the required physics a 3D model has been implemented for the HDD landfall, where the conductor follows the burial profile shown in Figure 4. Apart from the implemented geometry the two models are set up in the same manner.

The cross sectional bounds of the soil domain are 80 m wide by 60 m deep. Such soil dimensions are large enough to result in a minimal thermal gradient near the boundaries which negates any erroneous boundary effects due to the boundary condition, which could impact on the predicted conductor temperature.

To predict the temperature profile a coupled thermal-electrical model is required, where the electrical model defines the heat sources used to drive the temperature profile. It should be stressed that the thermal losses are nonlinear, due to the temperature dependent electrical resistivity of the armour, sheath and conductor. To reduce the complexity of these computational models, it is possible to calculate the electrical losses through the standard IEC 60287-1 method [5], and hence the model only needs to solve for the temperature profile. The FEA model calculates the steady state temperature profile using

$$\nabla[\kappa\nabla\theta] + Q = 0 \qquad [6]$$

Where κ is the thermal conductivity [$Wm^{-1}K^{-1}$], θ is temperature [K] and Q is the thermal losses [Wm^{-1}]. The heat transfer predicted by this equation is only due to thermal conduction, which is an accurate assumption for the solid domains considered in this model. The predicted thermal losses within the conductor, sheath and armour are uniformly distributed over the specific cable domains. This method retains the coupling between the temperature and electrical losses, by iteration of the thermal profile with corresponding temperature values being used to predict the electrical resistance and hence losses. This modelling approach has widely been used by previous publications [7].

Boundary conditions

Finally the boundary conditions for this model need to be defined. The soil surface is assumed to be a constant ambient temperature of 15 ºC. The bottom boundary of the model

is taken to be an isothermal temperature of 10 ºC. The vertical sides of the model are assumed to have a zero net heat flux across them due to their distance from the heat source i.e. the hot cable.

3.1.2 J tube models

To investigate the conductor thermal profile a 3D finite element model has been developed. Due to the variation in permissible heat flux from the cable to the ambient along its length, it is not possible to generate a 2D slice model. In keeping with the previous models, this numerical model only solves the thermal processes, as the electrical losses from the conductors, dielectrics, sheaths and armour are defined as heat sources according to the equations given in IEC 60287-1 [5].

The thermal conduction within the cable (solid domain) is solved using equation 6, above. Whilst the heat transfer within the cable is solely due to conduction, the space between the cable and the J tube contains a fluid, either water or air. Therefore additional heat transfer mechanisms need to be considered.

For the J tube water regions (i.e. below the sea level), there is an additional heat transfer due to convection in the water. However, due to the small distance between the cable and the J tube surface and due to the small thermal gradient; the convective currents within this region are not expected to be very strong. Furthermore, due to the relatively good thermal conductive nature of water, the convection heat transfer has been deemed negligible and so the water domain is modelled with only thermal conduction present. Given that the section in water is less thermally limiting than that in air, it is considered unlikely that this assumption will have any impact on the rating obtained.

Due to the poor thermal conductivity of air, the dominant heat transfer mechanism between the cable and the J tube cannot be assumed as conduction and so the convection and radiation must be considered. Instead of solving the Navier–Stokes equations, the natural convection is solved using an analytical heat transfer coefficient. Using such an approach, the convective heat transfer from the cable surface (q_{conv}) is proportional to the temperature difference between the cable surface (θ_{cable}) and the inner surface of the J tube (θ_{tube}). This convective heat sink is expressed by

$$q_{conv} = h_{conv}(\theta_{tube} - \theta_{cable}) \quad [7]$$

The thermal convection is solved using an analytical heat transfer method, where the heat transfer coefficient (h_{conv}) is defined by

$$h_{conv} = \frac{NuK_{air}}{\delta_g} \quad [8]$$

Where K_{air} is the thermal conductivity of the air and δ_g is the distance between the cable surface and the J tube inner wall. The empirically derived Nusselt number (Nu) for an annulus is defined by

$$Nu = 0.188Ra^{0.322}G^{-0.238}K^{0.442} \quad [9]$$

The Reynolds number (Ra) is defined by

$$Ra = \frac{Prg\beta(\theta_s - \theta_w)\delta^3}{\nu^2} \quad [10]$$

The geometric constants within this equation K and G are defined by

$$K = \frac{D_d}{D_e} \quad [11]$$

$$G = \frac{L_a}{\delta_g} \quad [12]$$

Where D_d and D_e are the cable diameter and inside diameter of the J tube in m. The length of the J tube air section is given by L_a.

To balance the convective heat sink on the cable surface and due to the closed nature of the J tube, the integral of convective heat from the cable surface is projected back on to the J tube inside surface.

The surface to surface radiation between the cable and J tube is defined by the temperature difference between the cable serving (θ_{cable}) and the inner surface of the J tube (θ_j) as by

$$q_{surface\,rad} = \varepsilon\sigma(\theta_j^4 - \theta_{cable}^4) \quad [13]$$

Where σ is the Stefan–Boltzmann constant (5.67 x10^{-8} $Js^{-1}m^{-2}K^{-4}$), ε is the surface emissivity, which is taken to be 0.9. Whilst the paint colour and finish does affect this, such an emissivity is a reasonable assumption.

External boundary conditions

With the internal physical processes defined, the external boundary conditions need to be specified. By initially considering the J tube below the sea level, the SoW states a maximum measured sea temperature to be 15 ºC. To reduce the computational complexity the surrounding sea domain is not modelled directly and instead the J tube surface below sea level is assumed to be at a constant temperature (θ_{water}). Such an assumption is reasonable due to the vast volume of water and the small continual tidal movement.

The external surface of the J tube air section and the exposed phases are considered to have both natural convection and surface to ambient radiation. Surface to ambient radiation is defined using equation 8, with the temperature difference instead being given by the outer surface of the J tube, $\theta_{j\,outer}$, and ambient, θ_{amb}. The external convection from the outer surface of the J tube to ambient is defined by equation 7, with the temperature difference being replaced by $\theta_{j\,outer} - \theta_{amb}$. The heat transfer coefficient from the outside surface of the J tube is also calculated using equation 8, with the ambient air temperature defined as 20 °C.

Both sections exposed to the air (J tube air section and exposed phases) also have to consider the solar heat flux. The solar heat flux (q_{solar}) and J tube absorptivity (α) are assumed to be 1000 Wm^{-2} and 0.4. Since the sun is a point in the sky, the total incident solar heat flux on a J tube should be given by a flat straight line perpendicular to the suns rays. Therefore the total solar energy which these models should consider is given by the integral of solar flux (product of solar heat flux and absorptivity) along the diameter of the J tube. This integral of heat flux is then uniformly distributed over the external surface of the tube.

3.2 Improved Models of Induced Losses

There is a widespread suggestion within the cable industry that the equations presently recommended within the IEC standard for armour losses in 3 core SL type cables (IEC 60287-1-1-2006+A1-2014, clauses 2.4.2.3.1 and 2.4.2.5) can overestimate the heat generated within the armour. Furthermore the standard IEC methods do not permit the assessment of armour loss reduction due to the use of alternate polymeric wires.

A recently published study has presented an updated thermal loss for a SL type cable [1].

For this method to be considered, the following additional cable parameters are required:

- Conductor lay length (assumed to be 2.3 m)
- Armour lay length of (assumed to be 4 m)
- Relative longitudinal permeability of the amour (μ_l) 870 (stated in [1])
- Relative transverse permeability of the amour (μ_t) 435 (stated in [1])

The relativity permeability of steel presented in IEC 60287-1 [5] (μ_l = 870 and μ_t = 10) was not used in this study, because the value presented there is for a composite steel/bitumen domain, rather than the pure steel permeability, which is required for these calculations. Using these above terms, a comparison of the predicted losses and loss factors given by this advanced method and the standard IEC method for the 800 mm^2 cable is presented in Figure 6 and Figure 7.

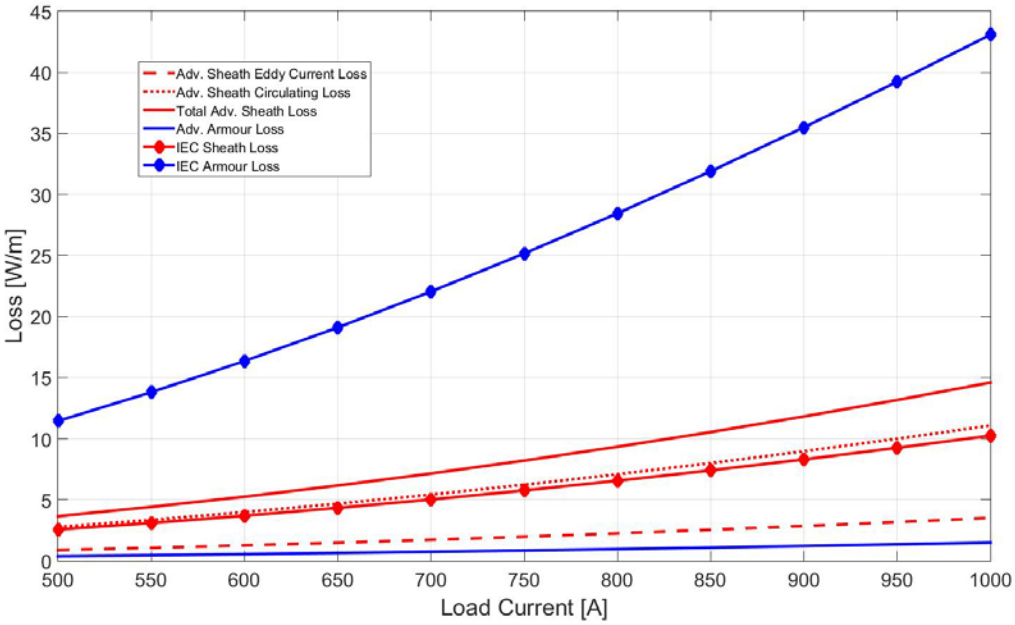


Figure 6 – Comparison of IEC and Advanced losses

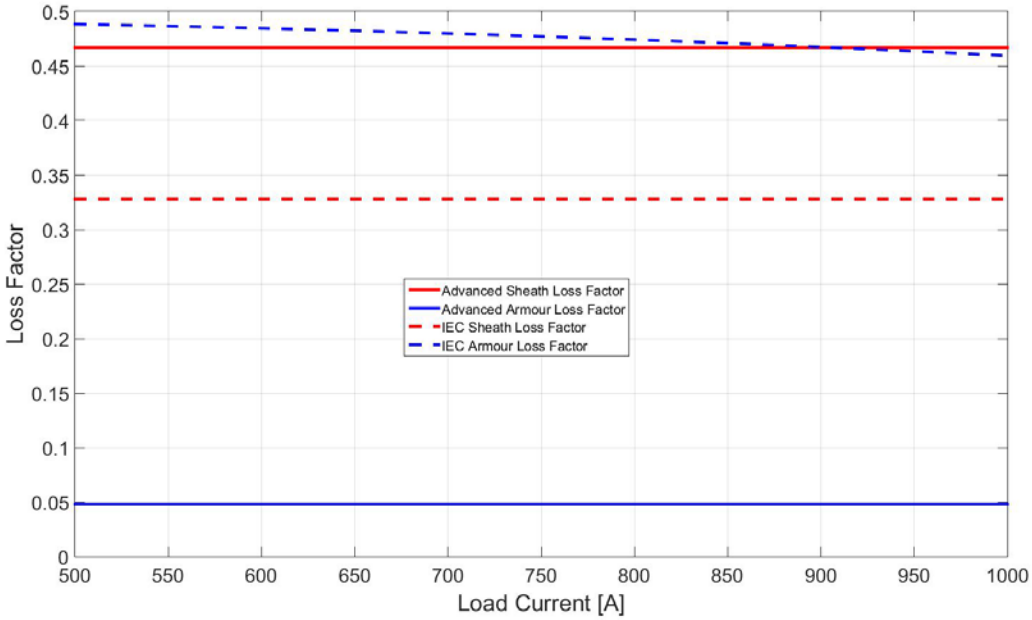


Figure 7 – Comparison of cable loss factors

From Figure 6 it is apparent that the IEC sheath losses are very similar to the circulating losses predicted by the new loss prediction method [1]. This would indicate that the IEC losses have not fully accounted for the possible contribution from eddy current within the sheath. Furthermore Figure 6 shows that the contribution of the eddy current losses are approximately 34% of the IEC 60287 sheath losses. By considering the above figures it is also apparent that the advanced losses predict a considerably lower armour loss than that given by IEC 60287. Whilst such a low value is possible, it is highly dependent on the permeability of the steel used in the armour.

We recommend that further investigation of armour wire permeability is undertaken, however the results given here are not considered to be significantly optimistic.

3.3 Discussion

The conductor temperature profile for both the HDD landfall model and the J tube model are shown in Figure 8 and Figure 9 respectively.

The conductor temperature profile for the HDD begins at a typical sea bed burial depth (x =0 m), after which the burial depth of the cable increases at the start of the landfall site. The cable remains at this deeper depth whilst within the landfall region, after which it returns to its initial burial depth. An indication of the cable profile is included within Figure 8. From this figure, it is apparent that there is a noticeable temperature increase as the depth of the buried cable increases to 10 m at the start of the landfall site. The increase in temperature is caused solely by the increased thermal resistance due to the greater burial depth. In the middle of the landfall site, there is a second increase in temperature, due to the assumed increase in soil thermal resistivity as one moves from the sea bed to the on-shore soil. Finally, once out of the landfall site, the temperature of the cable decreases due to the decreased burial depth. The final temperature on the on-shore side is greater than the initial temperature offshore, due to the increased soil thermal resistivity on the land. It is also apparent that the length of the deeply buried section is sufficiently long (for each region of soil thermal resistivity), such that the temperature in the center of the region is not affected by longitudinal heat transfer. This indicates that it would be possible to use a 2D model rather than a 3D model to predict the continuous thermal rating.

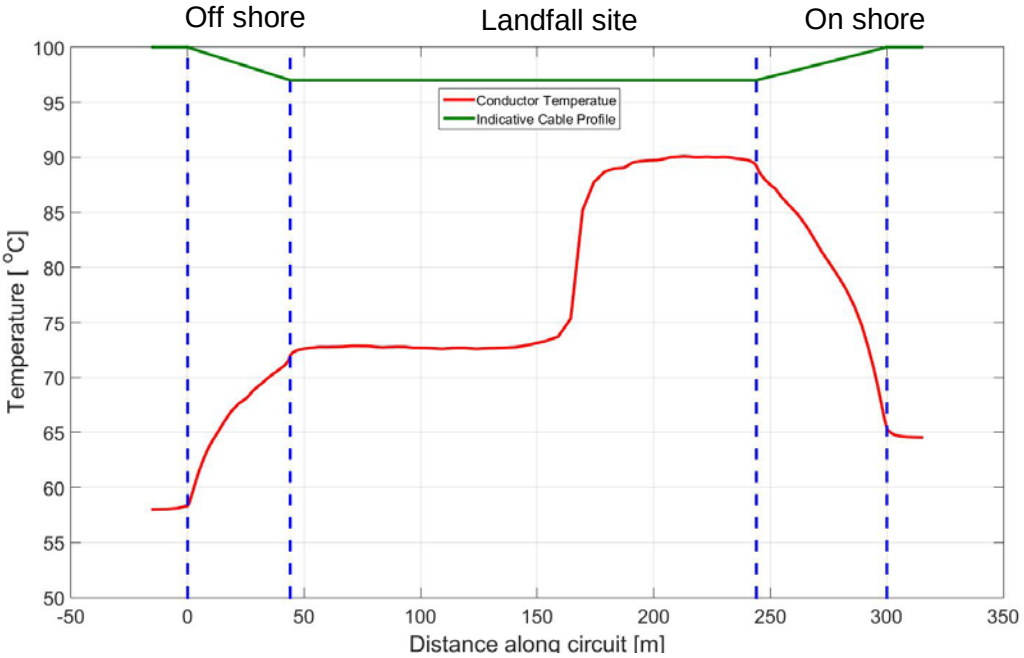


Figure 8 – Conductor temperature profile with HDD landfall at 644 A

The conductor temperature profile for the J tube (Figure 9) shows three distinct regions, which correspond to the three J tube sections presented in Figure 5. The hottest temperature within the J tube is observed within the air section. Starting at 10 m below the sea level (length equal to 0 m in Figure 9), the conductor temperature is approximately constant below the sea level due the isothermal boundary condition on the J tube water boundary. However as the tube air section approaches, the temperature begins to increase, due to longitudinal heat transfer from the hotter central region. The increase in temperature within the central region is caused by both an effective increase in thermal resistance between the cable surface and ambient, plus the addition of the solar heat flux. Within the tube air section, the temperature continues to rise up to a plateau. This temperature plateau is formed due to the diminishing longitudinal heat transfer from the hotter central J tube air section to the cooler neighbouring sections. The conductor temperature decreases once the phases have been separated due to the reduction in thermal resistance caused by the removal of the amour layer and cable fillers.

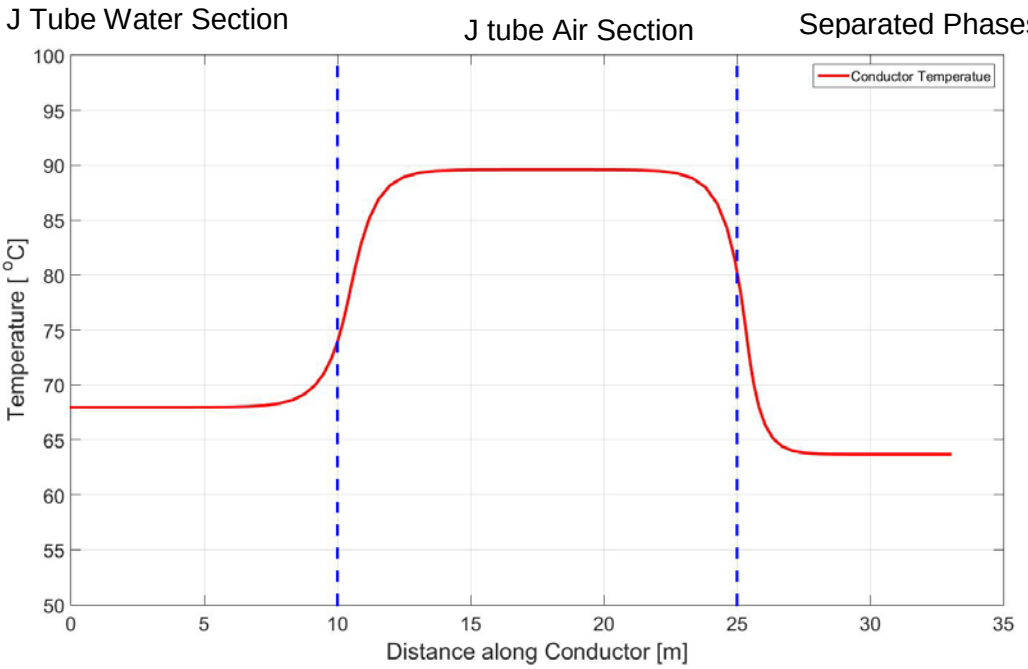


Figure 9 – Conductor temperature profile within J tube at 868 A

The numerical models outlined above have been used to calculate the continuous thermal rating for each environment with both the standard IEC losses and the advanced SL type losses presented in [1]. A comparison of the continuous seasonal ratings for the base case 800mm^2 132kV copper conductor is presented in Table 6.

Table 6 – Continuous seasonal ratings calculated by FEA

Environment	FEA with IEC losses [A]	FEA with advanced losses [A]
Typical seabed burial	893	925
Deep seabed burial	811	847
HDD landfall	605	644
J tube	893	928

The ratings of the larger cable sizes are presented in Section 4.0.

4.0 Continuous Ratings for Remaining Cables

The above sections have presented in detail the continuous ratings for an 800 mm^2 copper conductor in various installation environments with both the classical IEC and FEA approaches. This section presents the continuous thermal ratings for the remaining considered conductor sizes presented in Section 1.0. The continuous rating for these additional cables are calculated using the same methods and for the same installation environments as those considered in section 2 and 3.

4.1 Thermal Rating for remaining cables

The continuous thermal rating predicted by the standard analytical approaches for each of the installation environments are presented in Table 7. In this section the conductor sizes which are 2000 mm^2 are assumed to have an insulated Milliken design. By comparing the buried cable rating with 100% steel armour and 50% steel armour, it is apparent that the reduction in steel armour wires causes a decrease in rating. Whilst this is not what would be expected physically, the reason for this decrease is due to the implementation of the armour loss within IEC. Specifically the fact that the IEC method assumes the metal armour wires can be represented as a single annulus. Therefore a decrease in the number of armour wires reduces the annulus cross sectional area and hence increases the resistance of the annulus. This increase in resistance, causes an increase within the armour loss factor predicted by IEC.

Table 7 – Continuous rating from standard IEC approaches

Conductor	Voltage [kV]	IEC with 100% steel armour wires (A)			IEC with 50% steel armour wires (A)			
		Typical burial	Deeply burial	Landfall	Typical burial	Deeply burial	Landfall	ERA J tube (IEC losses)
1600 mm^2 Aluminium	220	968	864	623	939	837	602	900
2000 mm^2 Aluminium	220	1096	971	694	1054	932	664	1004
2000 mm^2 Copper	220	1206	1064	754	1152	1014	717	1076
2000 mm^2 Aluminium	275	1099	971	964	1055	929	661	991
2000 mm^2 Copper	275	1209	1063	752	1152	1010	712	1060

The continuous ratings in Table 7 show the same trend as that seen previously with the shallower the burial depth of the cable, the greater the continuous rating. Furthermore the J tube rating predicted by the ERA method is in between a deeply buried and landfall installation for all considered cable designs.

It should also be noted from Table 7, that for the same conductor size, there is a slight decrease in continuous rating with increased operating voltage. This is due to the slight increase in insulation thickness required at higher voltages, which results in a greater thermal resistance within the cable. Another reason for this rating decrease is because there is an increased dielectric thermal loss at higher operating voltages.

Before presenting the continuous rating for the advanced losses, the respective loss factors first need to be calculated for these cable designs, which are shown in Table 8.

Table 8 – Advanced loss factors

Conductor	voltage [kV]	Total no. armour wires	No. steel wires	Advanced Loss Factors	
				Sheath loss Factor (λ_1)	Armour loss Factor (λ_2)
1600 mm^2 Aluminium	220	130	65	0.45	0.07
2000 mm^2 Aluminium	220	146	73	0.7	0.11
2000 mm^2 Copper	220	146	73	1.06	0.17
2000 mm^2 Aluminium	275	152	76	0.77	0.12
2000 mm^2 Copper	275	152	76	1.2	0.18

The continuous ratings predicted by the FEA models for both IEC losses and the advanced losses are presented in Table 9. In this table the ratings are presented for cables which have 50% steel armour wires only. By considering the FEA ratings with IEC losses, it is apparent that they are slightly lower than the corresponding ratings predicted by a full IEC method, shown in Table 7. This trend is the same as that shown for the smaller 800 mm^2 conductor previously.

Table 9 – Continuous thermal rating of buried cables with FEA

Conductor	voltage [kV]	FEA with IEC losses (A)				FEA with Advance losses (A)			
		Typical burial	Deeply burial	Landfall	J tube	Typical burial	Deeply burial	Landfall	J tube
1600 mm^2 Aluminium	220	919	824	574	1036	1020	927	662	1076
2000 mm^2 Aluminium	220	1030	917	637	1116	1182	1066	761	1278
2000 mm^2 Copper	220	1130	1002	689	1253	1340	1205	857	1535
2000 mm^2 Aluminium	275	1024	910	634	1109	1160	1045	747	1255
2000 mm^2 Copper	275	1125	992	685	1224	1300	1168	833	1472

Table 9 shows that with the advanced losses the FEA ratings show a significant rating increase, as expected based on previous results. Further it is apparent that when comparing the continuous ratings between conductor sizes, the aluminum conductors have approximately an 8% lower rating with IEC losses and a 12% lower rating with advanced losses, as compared with the rating from a copper conductor.

It is again evident (from Table 9) that there is a slight decrease in rating between

comparable conductors (same cross sectional area and material) as the operating voltage is increased. This is expected, due to the greater thermal resistance caused by the thicker insulation and the increased dielectric loss due to the higher operating voltage.

4.2 Effect of Milliken Conductor Design

The previous conductor designs which are equal to or greater than 2000 mm^2 have been considered as insulated (oxidized) Milliken conductor design. This method is used to improve the rating by reducing the skin effect. The final part of this study determines the percentage rating impact on using such a conductor design over the plain stranded design.

To quantify the potential rating increase by using a Milliken conductor, the continuous rating of the 2000 mm^2 copper conductor at 275 kV will be considered over the entire range of installation environments. To account for the variation in conductor design (Milliken or plain stranded) the constants k_s and k_p given by IEC 60287-1 [5] need to be chosen accordingly (given in Table 4). Using these new values the updated advanced loss factors are:

- Plain stranded conductor, sheath loss factor (λ_1) is 0.82
- Plain stranded conductor, armour loss factor (λ_2) is 0.12

Both of these are a decrease in loss factor from the Milliken cable due to the higher conductor losses of a stranded conductor design. It should be noted that despite the significant change in loss factors the induced current in the sheath and armour is not significantly changed.

A comparison of the continuous rating with stranded and Milliken conductor design for the considered installation environments is presented in Table 10.

Table 10 - Rating comparison of stranded and Milliken conductor for 2000 mm^2 copper conductor at 275kV

Conductor	FEA IEC losses (A)				FEA advance losses (A)			
	Typical burial	Deeply burial	Landfall	J tube	Typical burial	Deeply burial	Landfall	J tube
Stranded	1039	923	642	1126	1180	1064	763	1228
Milliken	1125	992	685	1224	1300	1168	833	1472

From the above table it is apparent that the percentage rating increase for a Milliken conductor is slightly greater when using the advanced losses (maximum of approx. 9% at typical burial depth) than for the IEC losses (maximum of approx. 8% at typical burial depth). Furthermore it is evident that as the burial depth of the cable increases the percentage increase in rating, decreases. This is expected due to the increased dominance of the external soil on the rating as the depth increases.

5.0 Conclusions

This study has presented the continuous thermal rating for a thermally independent 132kV 800 mm^2 (plain stranded copper), three phase SL type cable in various different installations. The continuous ratings for these environments have been calculated using methods which increase in complexity from the standard IEC approaches to finite element analysis methods with advanced estimation of the induced losses. The predicted continuous ratings from each considered method and installation environment is presented in Table 11.

Table 11 – Comparison of continuous rating methods for 132kV 800mm^2 Cu

Installation environment	Continuous Ratings [A]			% gain between standard method and FEA with advanced losses
	Standard methods	FEA with IEC losses	FEA with advanced losses	
Typical seabed burial	896	893	925	3.2
Deep seabed burial	811	811	847	4.4
HDD Landfall	598	605	644	7.7
J tube	835	893	928	11

The above table shows that the HDD landfall always has the lowest continuous rating regardless of method. This section is therefore believed to be the most thermally limiting of the entire circuit.

By developing a bespoke FEA model and considering the advanced losses predicted by [1], there is a maximum 7.2% increase in rating from the standard IEC methods within the buried cables. Such a large increase in rating is apparent due to the considerable reduction in armour loss predicted by [1]. *Since the permeability of steel is dependent on the composition and manufacturing processes, it is suggested that the permeability is verified, as the armour loss factor will impact the continuous thermal rating.* It is further evident that the improvement in rating decreases as the burial depth of the cable decreases as the rating is dominated by the close proximity of the sea bed boundary.

There is a more significant increase in rating between the classical method and the bespoke FEA method for the J tube. This is caused by both the improved loss prediction and also the improved modelling of the heat transfer within a J tube, which the FEA model allows.

A summary of the continuous ratings for each of the larger cable design and all the considered cable installations is presented in Table 12. From this table it is evident that as the conductor cross sectional area increases for a given conductor material, there is as expected an increase in rating. The same trends in rating in regards to the installation environment follows that of the smallest conductor considered in detail above. Further it is apparent that when comparing the continuous ratings between conductor sizes, the aluminum conductors have approximately an 8% lower rating with IEC losses and a 12% lower rating with advanced losses, as compared with the rating from a copper conductor.

It should be noted that when using the IEC thermal losses, there is a decrease in rating by replacing half of the steel armour wires with polymer. This is believed not to be physical and is a limitation of the assumption made within the IEC approach. This issue is not present with the advanced losses as a rating increase has been observed. This further illustrates the importance of using the advance thermal losses for a SL type cable over the standard IEC approach.

Finally the study has shown that the percentage rating increase for a Milliken conductor is slightly greater when using the advanced losses (maximum of approx. 9% at typical burial depth) than for the IEC losses (maximum of approx. 8% at typical burial depth). Furthermore it is evident that as the burial depth of the cable increases the percentage increase in rating, decreases. This is expected due to the increased dominance of the external soil on the rating as the depth increases.

Table 12 – Complete summary of continuous thermal ratings for considered cables and installations

Conductor (plain stranded)	Voltage [kV]	IEC Method			ERA J tube (IEC losses)	FEA with IEC losses				FEA with Advance losses			
		Typical burial	Deeply burial	Landfall		Typical burial	Deeply burial	Landfall	J tube	Typical burial	Deeply burial	Landfall	J tube
800 mm^2 Copper	132	896	811	598	835	893	811	605	893	925	847	644	928
1600 mm^2 Aluminium	220	939	837	602	900	919	824	574	1036	1020	927	662	1076
2000 mm^2 Aluminium	220	1054	932	664	1004	1030	917	637	1116	1182	1066	761	1278
2000 mm^2 Copper	220	1152	1014	717	1076	1130	1002	689	1253	1340	1205	857	1535
2000 mm^2 Aluminium	275	1055	929	661	991	1024	910	634	1109	1160	1045	747	1255
2000 mm^2 Copper	275	1152	1010	712	1060	1125	992	685	1224	1300	1168	833	1472

6.0 References

[1] K. Goddard, J. A. Pilgrim, R. Chippendale and P. and Lewin, “Induced Losses in Three-core SL-type High Voltage Cables,” *IEEE Transactions on Power Delivery,* vol. 30, no. 3, pp. 1505-1513, 2015.

[2] CIGRE, “TB303: Revision of Qualification Procedures for HH and EHV Ac Extruded Underground Cable Systems,” CIGRE, 2006.

[3] IEC 60287-2-1 ed 2.0, “Electric cables - Calculation of the current rating - Part 2-1: Calculation of Thermal Resistance,” 2006.

[4] C. Long, Essential Heat Transfer, Longman; 1 edition , 1999.

[5] IEC 60287-1-1, “Electric cables - Calculation of the current rating: Part 1-1 Current rating equations (100% load factor) and calculation of losses - General,” 2006.

[6] M. Coates, “Rating cables in J tubes, report number 88-0108,” ERA technology, 1988.

[7] D. J. Swaffield, P. L. Lewin and S. Sutton, “Methods for rating directly buried high voltage cable circuits,” *IET Generation, Transmission & Distribution,* vol. 2, no. 3, pp. 393-401, 2008.

[8] R. A. Black and W. Z. Hartlein, “Ampacity of electric power cables in vertical protective rises,” *IEEE transaction on power apparatus and systems,* 1983.

7.0 Appendix

7.1 132kV 800 mm^2 copper conductor

Component	Material	Outer radius [mm]	Inner Diameter [mm]	Outer Diameter [mm]	Thickness [mm]
Conductor	Copper	17.2		34.5	
Conductor Screen	Semiconducting XLPE	18.7	34.5	37.5	1.5
Insulation	XLPE	35.7	37.5	71.5	17
Insulation screen	Semiconducting XLPE	37.2	71.5	74.5	1.5
Swelling Tape	Polymeric	38.7	74.5	77.5	1.5
Sheath	Lead alloy	41.2	77.5	82.5	2.5
Power core oversheath	Semiconducting PE	43.4	82.5	87.0	2.2
Filler	Polypropylene yarn				various
Binder tape	Fabric	95.5	187.0	191.0	2
Armour	Galvanised Steel	101.1	191.0	203.0	5.6
Outer serving	Polypropylene yarn	105.6	202.5	212.0	4.5

Additional Parameters	Value	unit
Conductor XSA	800	mm^2
Voltage	132	kV
Conductor material	Copper	
Conductor fill factor	0.86	
Tan(delta)	0.001	
Relative permittivity	2.5	
Voltage to earth, Uo	76210	V
Electric stress at conductor	6.30	kV/mm

Additional Parameters	Value	units
Capacitance per phase	0.21	µF/km
Inductance per phase	0.38	mH/km
Total number of armour wires	110	
Number of steel wires	110	
Number of polymeric wires	0	
Weight per power core	18.8	kg/m
Total cable weight per m	73.6	kg/m
Conductor AC resistance at 90 °C	3.12×10^{-5}	Ω/m

7.2 220kV 1600 mm^2 Aluminium conductor

Component	Material	Outer radius [mm]	Inner Diameter [mm]	Outer Diameter [mm]	Thickness [mm]
Conductor	Aluminium	24.3		49.0	
Conductor Screen	Semiconducting XLPE	25.8	49.0	52.0	1.5
Insulation	XLPE	45.8	52.0	92.0	20
Insulation screen	Semiconducting XLPE	47.3	92.0	95.0	1.5
Swelling Tape	Polymeric	48.8	95.0	98.0	1.5
Sheath	Lead alloy	51.8	97.67	104.0	3
Power core oversheath	Semiconducting PE	54.0	104.0	108.0	2.2
Filler	Polypropylene yarn	0.0			
Binder tape	Fabric	118.4	233.0	237.0	2
Armour	Steel	124.0	237.0	248.0	5.6
Outer serving	Polypropylene yarn	128.5	248.0	257.0	4.5

Additional Parameters	Value	units
Conductor XSA	1600	mm^2
Voltage	220	kV
Conductor material	Aluminium	
Conductor fill factor	0.86	
Tan(delta)	0.001	
Relative permittivity	2.5	
Voltage to earth	127017	V
Electric stress at conductor	8.6	kV/mm

Additional Parameters	Value	units
Capacitance per phase	0.24	µF/km
Inductance per phase	0.36	mH/km
Total number of armour wires	135	
Number of steel wires	135	
Number of polymeric wires	0	
Weight per power core	21.6	kg/m
Total cable weight per m	88.0	kg/m
Conductor AC resistance at 90 °C	2.73x10^{-5}	Ω/m

7.3 220kV 2000 mm^2 Aluminium conductor

Component	Material	Outer radius [mm]	Inner Diameter [mm]	Outer Diameter [mm]	Thickness [mm]
Conductor	Copper	27.2		54.5	
Conductor Screen	Semiconducting XLPE	28.7	54.5	57.5	1.5
Insulation	XLPE	48.7	57.5	97.5	20
Insulation screen	Semiconducting XLPE	50.2	97.5	100.5	1.5
Swelling Tape	Polymeric	51.7	100.5	103.5	1.5
Sheath	Lead alloy	54.7	103.5	109.5	3
Power core oversheath	Semiconducting PE	56.9	109.5	114.0	2.2
Filler	Polypropylene yarn	0.0			
Binder tape	Fabric	124.6	245.0	249.0	2
Armour	Steel/polymeric	130.2	249.0	260.5	5.6
Outer serving	Polypropylene yarn	134.7	260.5	269.5	4.5

Additional Parameters	Value	units
Conductor XSA	2000	mm^2
Voltage	220	kV
Conductor material	Aluminium	
Conductor fill factor	0.86	
Tan(delta)	0.001	
Relative permittivity	2.5	
Voltage to earth	127017	V
Electric stress at conductor	8.4	kV/mm

Additional Parameters	Value	units
Capacitance per phase	0.26	µF/km
Inductance per phase	0.34	mH/km
Total number of armour wires	142	
Number of steel wires	71	
Number of polymeric wires	71	
Weight per power core	23.8	kg/m
Total cable weight per m	96.3	kg/m
Conductor AC resistance at 90 °C	1.9 x10^{-5}	Ω/m

7.4 220kV 2000mm^2 copper conductor

Component	Material	Outer radius [mm]	Inner diameter [mm]	Outer Diameter [mm]	Thickness [mm]
Conductor	Copper	27.2		54.5	
Conductor Screen	Semiconducting XLPE	28.7	54.5	57.5	1.5
Insulation	XLPE	48.7	57.5	97.5	20
Insulation screen	Semiconducting XLPE	50.2	97.5	100.5	1.5
Swelling Tape	polymeric	51.7	100.5	103.5	1.5
Sheath	Lead alloy	54.7	103.42	109.5	3
Power core oversheath	Semiconducting PE	56.9	109.5	114.0	2.2
Filler	Polypropylene yarn				
Binder tape	Fabric	124.6	245.0	249.0	2
Armour	Steel/polymeric	130.2	249.0	260.5	5.6
Outer serving	Polypropylene yarn	134.7	260.5	269.5	4.5

Additional Parameters	Value	units
Conductor XSA	2000	mm^2
Voltage	220	kV
Conductor material	Copper	
Conductor fill factor	0.86	
Tan(delta)	0.001	
Relative permittivity	2.5	
Voltage to earth	127017	V
Electric stress at conductor	8.4	kV/mm

Additional Parameters	Value	units
Capacitance per phase	0.26	µF/km
Inductance per phase	0.34	mH/km
Total number of armour wires	142	
Number of steel wires	71	
Number of polymeric wires	71	
Weight per power core	36.6	kg/m
Total cable weight per m	134.8	kg/m
Conductor AC resistance at 90 °C	1.25 x10^{-5}	Ω/m

7.5 275kV 2000 mm^2 Aluminium conductor

Component	Material	Outer radius [mm]	Inner diameter [mm]	Outer Diameter [mm]	Thickness [mm]
Conductor	Copper	27.2		54.5	
Conductor Screen	Semiconducting XLPE	28.7	54.5	57.5	1.5
Insulation	XLPE	54.7	57.5	109.5	26
Insulation screen	Semiconducting XLPE	56.2	109.5	112.5	1.5
Swelling Tape	polymeric	57.7	112.5	115.5	1.5
Sheath	Lead alloy	60.7	115.5	121.5	3
Power core oversheath	Semiconducting PE	62.9	121.5	126	2.2
Filler	Polypropylene yarn	0.0			
Binder tape	Fabric	137.5	271.0	275.0	2
Armour	Steel/polymeric	143.1	275.0	286.5	5.6
Outer serving	Polypropylene yarn	147.6	286.5	295.5	4.5

Additional Parameters	Value	units
Conductor XSA	2000	mm^2
Voltage	275	kV
Conductor material	Aluminium	
Conductor fill factor	0.86	
Tan(delta)	0.001	
Relative permittivity	2.5	
Voltage to earth	158771	V
Electric stress at conductor	8.6	kV/mm

Additional Parameters	Value	units
Capacitance per phase	0.22	µF/km
Inductance per phase	0.51	mH/km
Total number of armour wires	157	
Number of steel wires	79	
Number of polymeric wires	78	
Weight per power core	27.1	kg/m
Total cable weight per m	110.3	kg/m
Conductor AC resistance at 90 °C	1.9 x10^{-5}	Ω/m

7.6 275kV 2000 mm^2 copper conductor

Component	Material	Outer radius [mm]	Inner diameter [mm]	Outer Diameter [mm]	Thickness [mm]
Conductor	Copper	27.2		54.5	
Conductor Screen	Semiconducting XLPE	28.7	54.5	57.5	1.5
Insulation	XLPE	54.7	57.5	109.5	26
Insulation screen	Semiconducting XLPE	56.2	109.5	112.5	1.5
Swelling Tape	polymeric	57.7	112.5	115.5	1.5
Sheath	Lead alloy	60.7	115.5	121.5	3
Power core oversheath	Semiconducting PE	62.9	121.5	126.0	2.2
Filler	Polypropylene yarn	0.0			
Binder tape	Fabric	137.5	271.0	275.0	2
Armour	Steel/polymeric	143.1	275.0	286.5	5.6
Outer serving	Polypropylene yarn	147.6	286.5	295.5	4.5

Additional Parameters	Value	units
Conductor XSA	2000	mm^2
Voltage	275	kV
Conductor material	Copper	
Conductor fill factor	0.86	
Tan(delta)	0.001	
Relative permittivity	2.5	
Voltage to earth	158771	V
Electric field stress at conductor	8.6	kV/mm

Additional Parameters	Value	units
Capacitance per phase	0.22	µF/km
Inductance per phase	0.51	mH/km
Total number of armour wires	157	
Number of steel wires	79	
Number of polymeric wires	78	
Weight per power core	40.0	kg/m
Total cable weight per m	148.8	kg/m
Conductor AC resistance at 90 °C	1.25 x10^{-5}	Ω/m

Appendix B:

The scope of work required the total thermal loss of the cable (Q [W/m]**)** to be given with respect to the rated current (I [A]) and the total cable resistance (electrical), expressed in the following form

$$Q = 3I^2 R_x \qquad \text{B.1}$$

Since the current within the sheath and the armour are different to that within the conductor, an “equivalent term” is required to represent modified resistance in the sheath and armour. By summing the conductor ac resistance with equivalent term for the sheath and armour, the total equivalent term ‘R_x’ is obtained.

It should also be noted that the electrical resistance and hence the thermal losses are temperature dependent. Whilst the temperature of the conductor under continuous rating conditions is trivial to determine (90 °C) the thermal profile within the cable and hence the temperature of the sheath and armour is installation dependent. To remove this uncertainty the values presented in Table 13 are for the typical burial case, used in the above studies.

Table 13 – Total cable thermal loss

Cable Design	Continuous Rating [A]	Conductor AC Resistance at 90 °C [Ω/m]	Equivalent term		Total equivalent term (R_x)	Total loss (Q) [W/m]
			sheath	armour		
800 mm^2 Copper	893	3.12E-05	8.74E-06	1.59E-05	5.58E-05	134
1600 mm^2 Aluminium	919	2.70E-05	1.16E-05	1.84E-05	5.70E-05	144
2000 mm^2 Aluminium	1030	1.80E-05	1.28E-05	1.80E-05	4.88E-05	155
2000 mm^2 Copper	1130	1.19E-05	1.26E-05	1.82E-05	4.27E-05	164
2000 mm^2 Aluminium	1024	1.80E-05	1.40E-05	1.78E-05	4.99E-05	157
2000 mm^2 Copper	1125	1.20E-05	1.39E-05	1.80E-05	4.39E-05	167

The authors of this report would like to stress these values are for single installations and sets of environmental conditions and care should be taken if they are to be used for a different case.